Electronic Supplementary Information for

Getting the details right: optical, dielectric, and vibrational outcomes of structural phase transition in one-dimensional pyrrolidinium lead iodide and the role of defects

Katarzyna Fedoruk[1], Szymon J. Zelewski[2,3], Jan K. Zaręba[4], Maciej Ptak[5], Mirosław Mączka[5], Adam Sieradzki[1]

[1]Department of Experimental Physics, Faculty of Fundamental Problems of Technology, Wrocław University of Science and Technology, Wybrzeże Wyspiańskiego 27, 50-370 Wrocław, Poland

[2]Department of Semiconductor Materials Engineering, Faculty of Fundamental Problems of Technology, Wrocław University of Science and Technology, Wybrzeże Wyspiańskiego 27, 50-370 Wrocław, Poland

[3]Cavendish Laboratory, JJ Thomson Avenue, University of Cambridge, Cambridge CB3 0HE, United Kingdom

[4]Advanced Materials Engineering and Modelling Group, Faculty of Chemistry, Wrocław University of Science and Technology, 50-370 Wrocław, Poland

[5]Institute of Low Temperature and Structure Research, Polish Academy of Sciences, 50-422 Wrocław, Poland

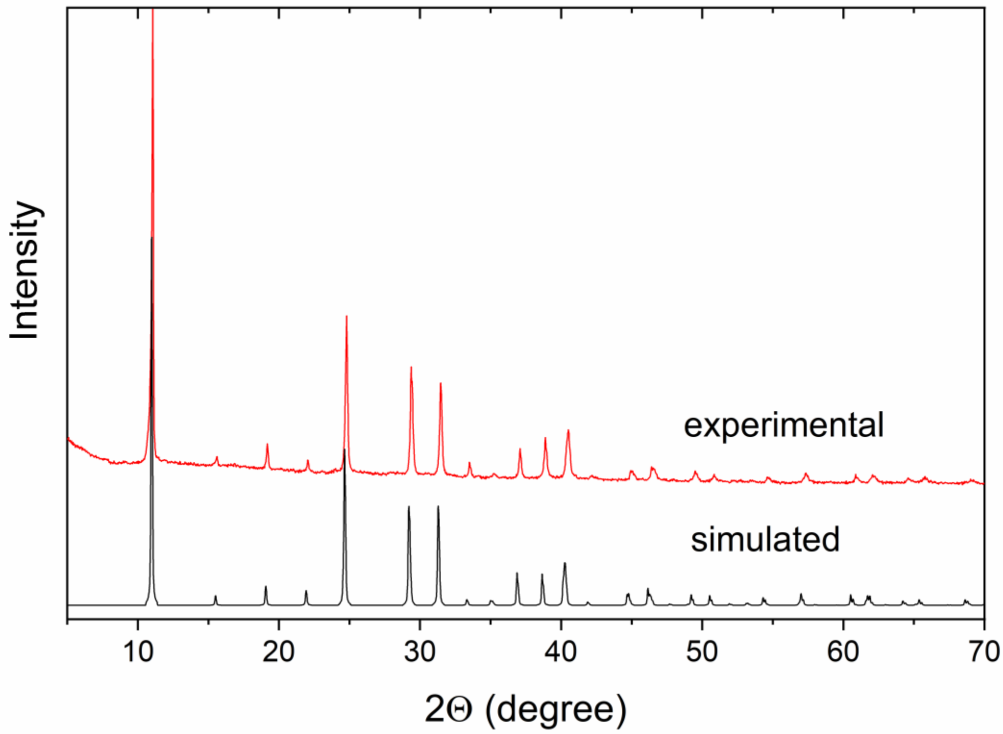

Figure S1. Comparison of powder XRD pattern of $PyrPbI_3$ with the calculated one based on the room-temperature single-crystal data reported previously.

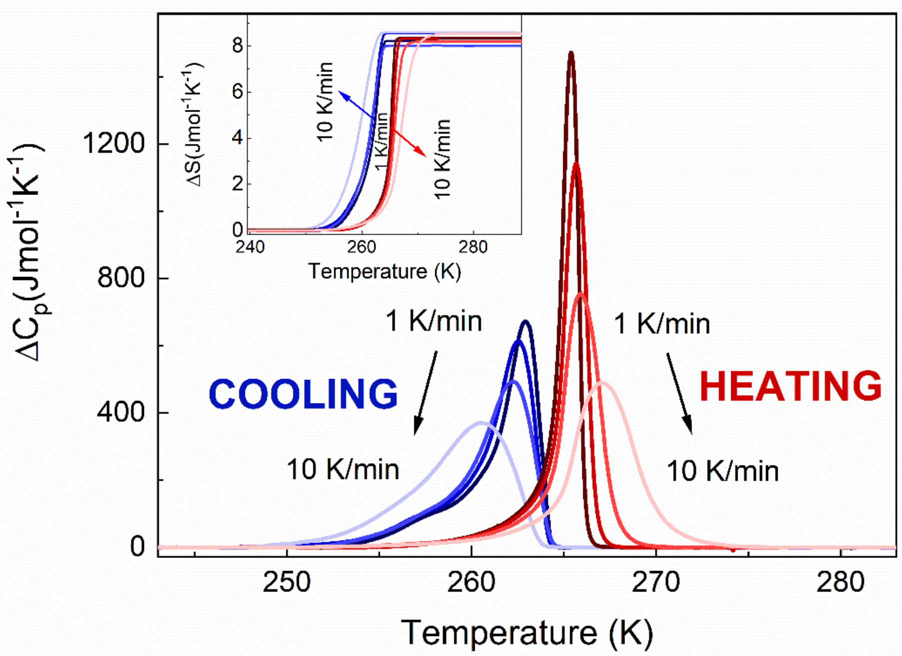

Figure S2. Temperature dependence of excess heat capacity, ΔC_p, obtained for heating and cooling cycles of $PyrPbI_3$ with the rates equal 1, 2, 5, and 10 K min^{-1}. The inset shows the corresponding change of entropy, ΔS, measured in the same conditions.

Table S1. Tentative assignments of Raman bands at 80 and 300 K.

LT phase, 80 K (cm^{-1})	HT phase, 300 K (cm^{-1})	Assignment
3119w	3185sh	$\nu_{as}NH_2$
3065w	3080vw	$\nu_{s}NH_2$
3001s, 2983s, 2960s, 2955sh, 2935s,	3004m, 2981s, 2964s, 2952sh, 2931s	$\nu_{as}CH_2$
2900m, 2883sh, 2878m	2898m, 2887m, 2874m	$\nu_{s}CH_2$
1550m	1560w	δNH_2
1473w, 1452sh, 1447m	1468w, 1452sh, 1445m	δCH_2
1369w, 1353m	1353w	ωNH_2
1324vw, 1306w, 1285w	1308w	$\omega CH_2+\omega NH_2$
1235m	1228w	τCH_2
1196	1199w	τNH_2
1051m, 1016w, 977w, 905m	1046w, 1011w, 982vw, 905m	$\rho CH_2+\nu$(ring)
868m	863m	ρNH_2
570w	567w	$\delta(\text{ring})_{ip}$
274m	272w	$\delta(\text{ring})_{op}$
133vs, 102m	140sh, 105vs	$\nu PbI_6+\delta PbI_6$

Key: ν, stretching; ν_s, symmetric stretching; ν_{as}, antisymmetric stretching; δ, bending; ω, wagging; τ, twisting; ρ, rocking; ip, in-plane; op, out-of-plane; vs, very strong; s, strong; m, medium; w, weak; vw, very weak; sh, shoulder.

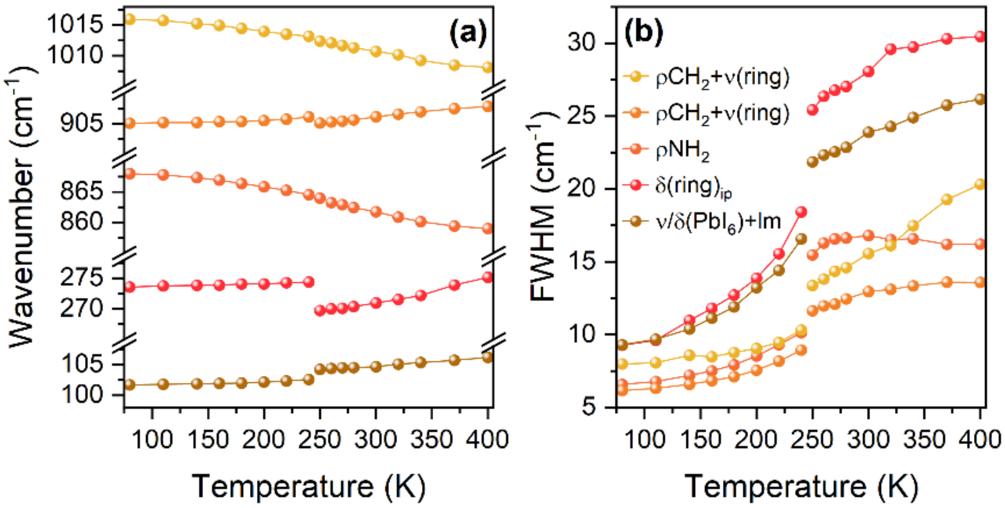

Figure S3. Temperature dependence of energy and broadening (FWHM values) for selected Raman bands.

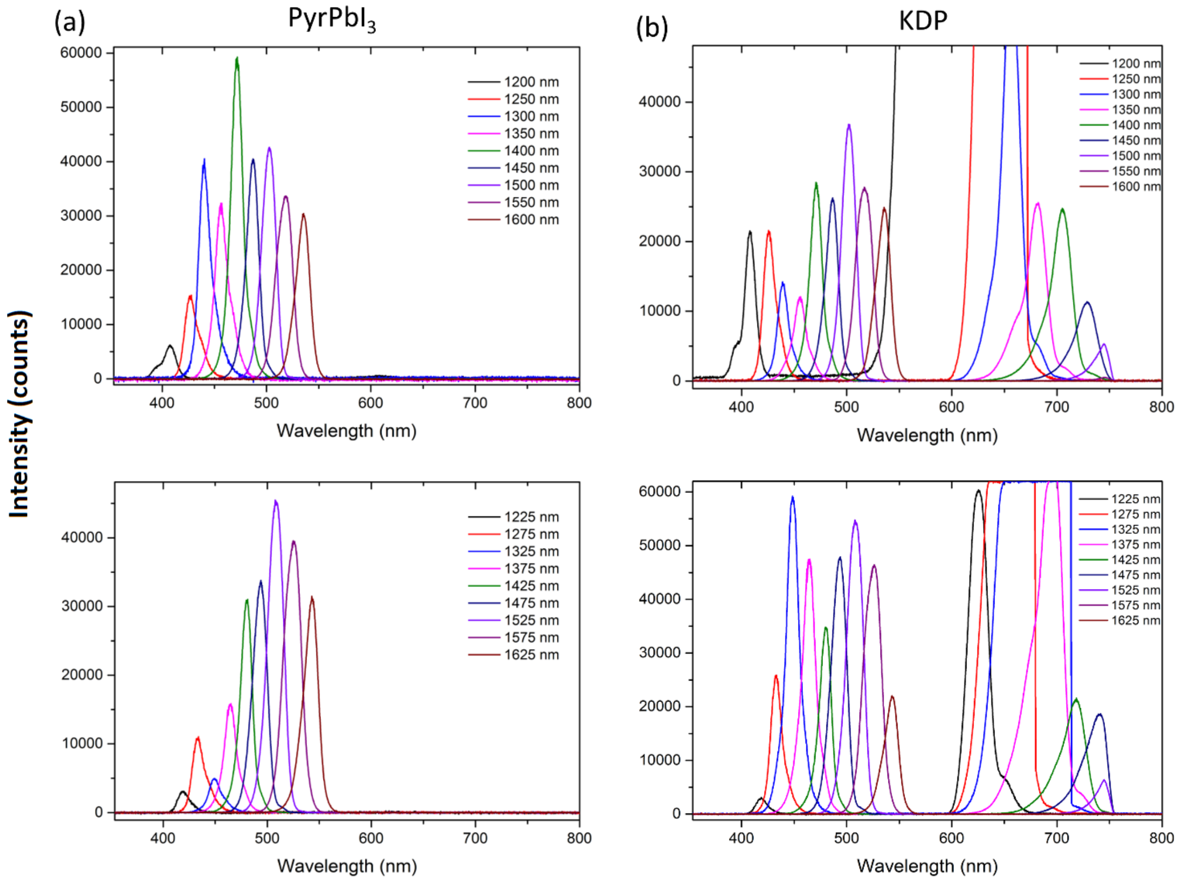

Figure S4. Experimental spectra of nonlinear emissions obtained upon irradiation with femtosecond laser pulses from 1200 nm to 1625 nm of (a) $PyrPbI_3$ and (b) KDP. Spectra have been divided into two subsets to improve clarity. It is shown that for $PyrPbI_3$ only THG response is registered, confirming its centrosymmetry, whereas KDP shows simultanously THG and SHG responses. Note that the spectra have been measured for various collection times ranging from 40 ms to 5000 ms, and are not normalised to the same collection time in this plot. T = 293 K.

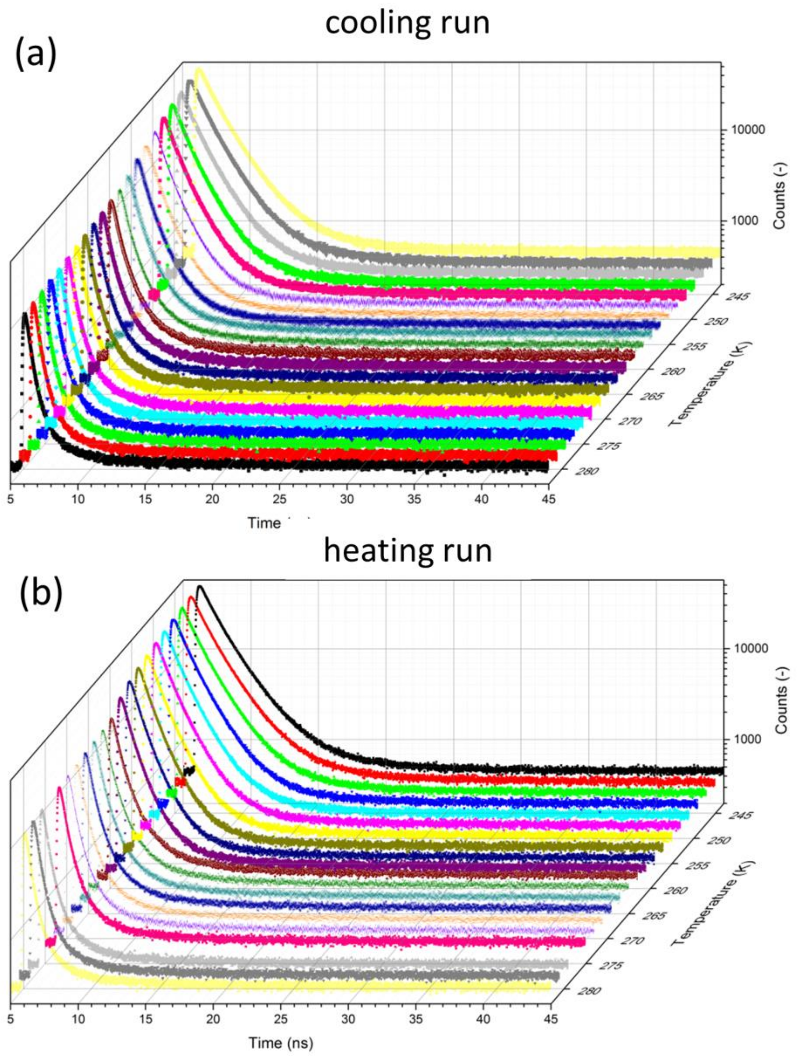

Figure S5. Luminescence decay curves for (a) cooling (283 K – 243 K) and (b) heating (243 K – 283 K) run. λ_{ex} = 375 nm, λ_{em} = 660 nm.

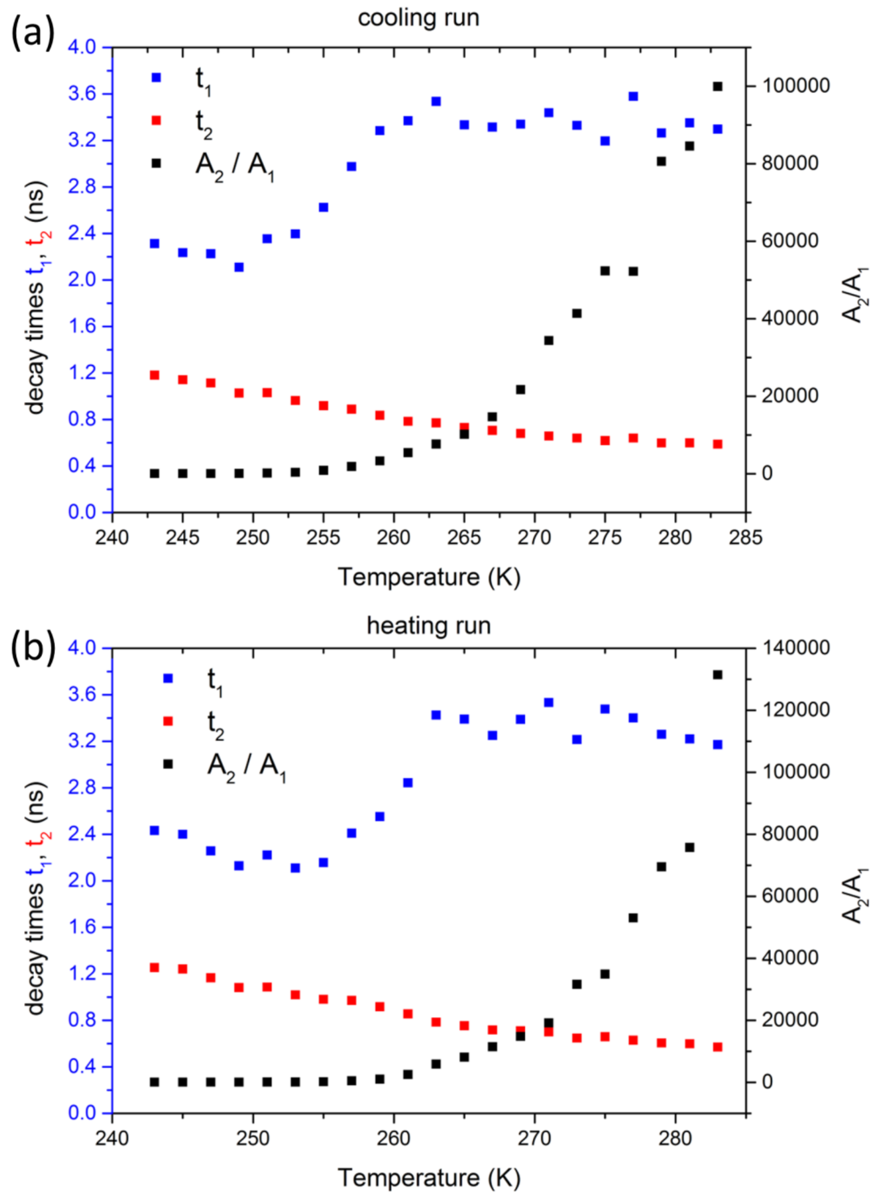

Figure S6. Temperature plots of luminescence decay time components τ_1 and τ_2 and corresponding weight ratios (A_2/A_1) for (a) cooling (283 K – 243 K) and (b) heating (243 K – 283 K) run. λ_{ex} = 375 nm, λ_{em} = 660 nm.